Environmental Pollution 341 (2024) 122968

Contents lists available at ScienceDirect

Environmental Pollution

journal homepage: www.elsevier.com/locate/envpol

Titanium-doped PET nanoplastics, from opaque milk bottle degradation, as a model of environmental true-to-life nanoplastics. Hazardous effects on *Drosophila*☆

Mohamed Alaraby [a,b], Aliro Villacorta [a,c], Doaa Abass [a,b], Alba Hernández [a], Ricard Marcos [a,*]

[a] Group of Mutagenesis, Department of Genetics and Microbiology, Faculty of Biosciences, Universitat Autònoma de Barcelona, Cerdanyola del Vallès, Spain
[b] Zoology Department, Faculty of Sciences, Sohag University (82524), Sohag, Egypt
[c] Facultad de Recursos Naturales Renovables, Universidad Arturo Prat, Iquique, Chile

ARTICLE INFO

Keywords:
True-to-life nanoplastics
Internalization pathway
Oxidative stress
Gene expression genotoxicity
Drosophila melanogaster

ABSTRACT

Micro and nanoplastics (MNPLs) are emergent environmental pollutants, resulting from the degradation of plastic waste, requiring urgent information on their potential risks to human health. To determine such risks, reliable true-to-life materials are essential. In this work, we have used titanium-doped PET NPLs [PET(Ti)NPLs], obtained by grinding opaque milk polyethylene terephthalate (PET) bottles, as a true-to-life MNPLs model. These opaque PET bottles, with an average size of 112 nm, contain about 3% Ti in the form of titanium dioxide rod nanoparticles. TEM investigation confirmed the mixed Ti/PET nature of the obtained true-to-life NPLs, and the rod shape of the embedded TiO_2NPs. In the *in vivo Drosophila* model neither PET(Ti)NPLs nor TiO_2NPs reduced the survival rates, although their internalization was confirmed in different compartments of the larval body by using confocal and transmission electron microscopies. The presence of Ti in the PET(Ti)NPLs permitted to quantify its presence both in larvae (2.1 ± 2.2 μg/g of Ti) and in the resulting adults (3.4 ± 3.2 μg/g of Ti) after treatment with 500 μg/g food of PET(Ti)NPL, suggesting its potential use to track their fate in more complex organisms such as mammals. PET(Ti)NPLs, as well as TiO_2NPs, altered the expression of genes driving different response pathways, inducing significant oxidative stress levels (up to 10 folds), and genotoxicity. This last result on the genotoxic effects is remarkable in the frame of the hot topic discussion on the risk that titanium compounds, used as food additives, may pose to humans.

1. Introduction

The high production/use of plastics is paired with the generation of increasing levels of environmental plastic waste pollution. Once in the environment, plastic wastes are submitted to direct and indirect stress of various abiotic and biotic interactions which rips large plastic pieces into micro- and nanoplastic (MNPLs) particles (Su et al., 2022). The increased environmental presence of MNPLs has moved researchers to design experiments aiming to identify, quantify, and evaluate the potential hazards posed by MNPLs. Nevertheless, due to the lack of representative MNPL, most of the studies have been carried out using commercial pristine polystyrene MNPLs. Although this practical but unrealistic material has permitted to lay the groundwork for the potential mechanisms of MNPL hazards, their extension to more representative true-to-life MNPLs is required. These true-to-life MNPLs are obtained by degrading plastic goods in the lab using different approaches. Thus, by sanding water polyethylene terephthalate (PET) plastic water, PET MNPLs were obtained (Villacorta et al., 2022); similarly, by grinding chewing gum high-density polyethylene (HD-PE) plastic bottles, single-use polypropylene (PP) beverage glasses, and polystyrene (PS) cutlery items, the three types of MNPLs were obtained (Marchesi et al., 2023). Although the current approaches to producing true-to-life MNPLs may not completely reflect those mechanisms taking place in nature (their production is subjected to long-term exposures and interaction with several factors), they present a step forward toward exploring the expectable potential impacts of environmental MNPLs

☆ This paper has been recommended for acceptance by Dr Hefa Cheng.

* Corresponding author. Group of Mutagenesis, Department of Genetics and Microbiology, Faculty of Biosciences, Universitat Autònoma de Barcelona, Campus of Bellaterra, 08193 Cerdanyola del Vallès (Barcelona), Spain.
E-mail address: ricard.marcos@uab.cat (R. Marcos).

https://doi.org/10.1016/j.envpol.2023.122968
Received 23 August 2023; Received in revised form 22 October 2023; Accepted 14 November 2023
Available online 16 November 2023

(Ducoli et al., 2022).

One important aspect to highlight of true-to-life MNPLs is that they contain those additives initially incorporated during the production of plastic goods, including food packages. Although the presence of metal additives is strongly dependent not only on the type of plastic but also on the intended use, the presence of titanium in opaque PET plastic bottles used to pack milk is around 3% (Villacorta et al., 2023). The addition of Ti, mainly in the form of rod TiO_2NPs, provides the light protection required by ultra-high-temperature (UHT) milk and minimizes gas permeability.

Aiming to obtain true-to-life MNPLs opaque PET milk bottles have been recently used as a source, and their physicochemical properties have been extensively characterized (Villacorta et al., 2023). Interestingly the obtained MNPLs showed TiO_2NPs intruded in the PET matrix and these complexes were stable both in dispersion and internalized into cells. For these reasons, they have been proposed as an appropriate material to determine the fate of MNPLs in complex organisms like mammals. As a true-to-life MNPL model, the obtained PET(Ti)NPLs would overcome the problems of synthetic metal-doped nanoplastics proposed to such end (Mitrano et al., 2019; Clark et al., 2022).

Despite the potential usefulness of PET(Ti)NPLs in tracking the fate of ingested/inhaled MNPLs in tissues and organs, their hazardous impacts should not be overlooked. The complex metal-MNPLs can modify the toxicological profiles of each component separately, as demonstrated for silver and polystyrene NPLs in human intestinal Caco-2 cells (Domenech et al., 2021) and in *Drosophila* (Alaraby et al., 2022b); and in arsenic and polystyrene NPLs co-exposures, where oncogenic biomarkers were exacerbated under an *in vitro* long-term exposure scenario (Barguilla et al., 2022). Although no previous studies have been done using TiO_2NPs/MNPLs complexes, it should be remembered that concerns about genotoxicity and accumulation of TiO_2NPs after ingestion in the body cannot be ruled out (EFSA, 2021).

To get sound information on the potential hazards associated with PET-Ti-NPLs exposure we have used *Drosophila melanogaster,* as a well-known multifunctional *in vivo* model (Alaraby et al., 2022b). *Drosophila* has a mammalian-like intestinal system with a clear microbiota, a fat body resembling liver-equivalent oenocytes, and a genome with high gene homology (60%) related to human diseases (Rubin et al., 2000; Reiter et al., 2001). At the level of blood cells, plasmatocytes of *Drosophila* (95% of the hemocytes), play a role in phagocytosis, tissue remodeling, and cellular immune responses, like human macrophages, and crystal cells and lamellocytes perform functions analogous to clotting and granuloma formation (Buchon et al., 2014). Accordingly, we have used *Drosophila* to understand the internalization of PET(Ti)NPLs after oral administration. Furthermore, changes in the gene expression of a wide set of genes involved in different functions, as well as oxidative stress, and genotoxicity induction were determined. TiO_2NPs effects were also evaluated in parallel for comparisons.

2. Materials and methods

2.1. PET(Ti)NPLs obtention

PET(Ti)NPLs were produced as indicated in the recent publication of Villacorta et al. (2023). In summary, small pieces (12 cm^2) of opaque milk bottles were ground with a diamond rotary burr accessory, and the generated dust was sieved, dispersed in a heated (50 °C) trifluoroacetic acid solution, stirred, and centrifuged. The obtained pellets were resuspended in 0.5% sodium dodecyl sulfate, vigorously mixed, ultrasonicated, and finally, 1 mL aliquots were immediately frozen on cryotubes in liquid nitrogen and stored at −80 °C until further use. TiO_2NPs nanorods, as those used in the preparation of opaque PET materials, were obtained from Chemours Company (Kallo, Belgium).

2.2. PET(Ti)NPLs characterization

To determine morphology, size, and degree of aggregations, a transmission electron microscopy (TEM, JEOL JEM 1400 instrument. Tokyo, Japan) was used. TEM, working at 200 kV with energy-dispersive X-ray spectroscopy (EDX), was used to detect titanium doped inside the PET matrix. To pinpoint the behavior (Brownian movement and tendency to aggregate) of PET(Ti)NPLs or TiO_2NPs in suspension, a Zetasizer® Ultra device from Malvern analytical (Cambridge, United Kingdom) was selected to measure their dynamic light scattering (DLS) and the Zeta potential. Fourier transform infrared spectroscopy (FTIR) was used to identify the chemical composition (functional groups) to confirm the polymer type (PET). To perform FTIR, a drop of the dispersion was placed on a gold mirror and let dry for one week inside a Petri dish and analyzed by a Vertex 80 device (Bruker Corporation, Billerica, Massachusetts, USA).

2.3. Drosophila melanogaster (experimental design)

2.3.1. Egg-to-adult viability

The Canton-S strain was used in the experiments aiming to determine the potential toxicity of PET(Ti)NPLs and TiO_2NPs. Flies were kept at 24 ± 0.5 °C and a 65 ± 5% relative humidity, with a 12 h light/dark cycle, and fed with a standard medium. To proceed, eggs of Canton-S (6 h) were counted and transferred into a treated instant medium (Carolina Biological Supply Co., Burlington, NC). The treated medium contains 4 g of dehydrated medium wetted with 10 mL of different concentrations of PET(Ti)NPLs and TiO_2NPs (12.5, 50, and 200 μg/mL food) equivalent to (31.5, 125, and 500 μg/g food). The survival rates were determined by counting the emerged adults from the treated media in comparison with untreated ones (Milli-Q water hydrated medium). The experiments were carried out with five replicates (50 eggs/vial) for each dose. In addition, the emerged adults were carefully checked to detect any type of morphological changes.

2.3.2. Internalization analysis

(i) **Transmission electron microscopy investigation:** To follow PET(Ti)NPLs and TiO_2NPs' internalization fate inside *Drosophila* larvae, our previous protocol was followed (Alaraby et al., 2022a). To proceed, midguts of 3rd instar larvae were extracted in phosphate buffer (PB; 0.1 M, pH 7.4), and fixed for 2 h in a solution containing 4% paraformaldehyde and 1% glutaraldehyde in 0.15 M phosphate buffer, pH 7.4. For post-fixation and staining, midgut tissues were treated with 1% (w/v) osmium tetroxide containing 0.8% (w/v) potassium hexacyanoferrate for 2 h, followed by four washes with deionized water and sequential dehydration in acetone. The fixed tissues were embedded in Eponate 12TM resin (Ted Pella Inc., Redding, CA) and left to polymerize at 60 °C for 48 h. Trypan blue-stained semi-thin sections were investigated to determine the adequate midgut regions for ultrathin sections (100 nm thickness). Ultrathin sections were cut with a diamond knife (450, Diatome, Biel, Switzerland), mounted upon non-coated 200 mesh copper grids, and contrasted with conventional uranyl acetate (30 min) and Reynolds lead citrate (5 min) solutions, respectively. Finally, the high contrast transmission electron microscopy TEM (JEOL 1400, 120 kV) was used to detect the presence of PET(Ti)NPLs and TiO_2NPs in the different compartments (gut lumen, intestinal barrier, and hemolymph).

(ii) **Confocal microscopy:** The internalization of labeled PET(Ti)NPLs in different tissues of *Drosophila* was investigated using a Leica TCS SP5 confocal microscope, with an excitation wavelength of 561 nm, and emission between 580 and 700 nm. To label PET(Ti)NPLs from the surrounding biological tissues and fluids, the textile-specific natural fluorescent dye (iDye poly Pink)

was used (Villacorta et al., 2023). Briefly, 10 mg of iDye was added to 1 mL of PET(Ti)NPLs (5 mg/mL), vigorously vortexed, and incubated for 2 h at 70 °C on a glass tube. The stain-particles suspension was left for 1 h at room temperature, then diluted with 9 mL Milli-Q water, and centrifuged at 4000 rpm on an Amicon® Ultra-15 centrifugal Ultracel®-100 K filter 1 × 10 5 MWCO for 15 min. Four days treated larvae with stained PET(Ti) NPLs (500 μg/g food) were dissected with 1% PBS, and samples of larval tissues and hemolymph were collected for confocal visualization. Hoechst 33,342 (excitation of 405 nm and emission collected at 415–503) will be used to stain nuclei (blue colored) (0.5 μL/1 mL), while Cellmask (excitation of 633 nm and emission collected at 645–786) was used to stain cell membranes (red color). Hoechst 33,342 and Cellmask concentration was 0.5 μL for 1 mL samples. The reflection property will be used for the detection of metal hybrid MNPLs.

2.3.3. Internalized titanium (Ti) quantification

The amount of titanium internalized was quantitatively determined in two different developmental stages (larvae and adults) after PET(Ti) NPLs and TiO_2NPs exposure. *Drosophila* larvae were divided into two groups. In the first group, the treated larvae (PET(Ti)NPLs or TiO_2NPs) were collected after 120 h (five days) and stored at −80 °C. In the other group larvae, whether treated with PET(Ti)NPLs or TiO_2NPs, were collected at 96 h of exposure (four days) and transferred into a new clean untreated medium for 24 h to completely clean their midgut from the treated medium, then collected again and stored like the previous group. To determine the Ti content in adults, exposed larvae were allowed to continue their development until reach the adult stage. The treated adults were collected and stored for quantification analysis. The experiment was carried out in five replicates, and untreated samples were used as the negative control. The Ti content in untreated and treated medium was determined to confirm the initial amount of Ti in food. The samples (larvae, adults, and food medium) were incubated at 70 °C overnight to dry, weighed, and digested with a mixture of HNO_3 and HF in a microwave oven for 1 h at 270 °C under high-pressure conditions. The digested samples were diluted in HNO_3 (1% v/v) with a final volume of around 10 mL and weight. The Ti concentration was detected using an Agilent Model 7900 Inductively Coupled Plasma Mass Spectrometer (ICP-MS).

2.3.4. Gene expression analysis by real-time PCR

Changes in the expression levels of various genes, representative of different regulatory-respond pathways, were analyzed. The pooled genes included the Heat shock protein-70 (*Hsp70)*, catalase (*Cat*) and Cu, Zn superoxide dismutase (*Sod2*), 8-oxoguanine DNA glycosylase (*Ogg1*), dual oxidase (Duox), and peritrophin-A (*Peri*) (Alaraby et al., 2015). The list of used primers for the studied genes is indicated in the supplementary material (Table S1). Larvae were homogenized in TRIzol® Reagent (Invitrogen, Carlsbad, CA), and the total RNA was extracted according to the manufacturer's procedures, quantified using a NanoDrop 1000 spectrophotometer, and treated with RNase-free DNase to remove DNA contamination. RNA samples (2000 ng) were reversely transcribed into cDNA, using the Transcriptor First Strand cDNA Synthesis Kit (Roche), following the manufacturer protocol, and were kept at −20 °C until use. Furtherly, cDNA was polymerized by Quantitative PCR using a LightCycler® 480 SYBR Green I Master (Roche, Mannheim, Germany). The cycling conditions were 95 °C for 1 min, followed by 55 cycles of 95 °C for 1 min, and 65 °C for 30 s. Cycle threshold (Ct) values were calculated with the LightCycler software in comparison with untreated controls.

2.3.5. Oxidative stress determination

ROS levels were evaluated in hemocytes of four days larvae (~50 larvae are pooled from triplicate per dose) (Alaraby et al., 2018). PET (Ti)NPLs and TiO_2NPs treated larvae, as well as unexposed ones, were dissected in 1% PBS, and incubated with 5 μM 6-carboxy-2,7′-dichlorodihydro-fluorescein diacetate (DCFH-DA) at room temperature. Ten fluorescent images were picked up using a fluorescent microscope with an excitation of 485 nm and an emission of 530 nm (green filter) to investigate fluorescent hemocytes (containing high ROS levels). The quantitative analysis of the fluorescent images was performed using the ImageJ program. The obtained data of treated larvae were compared with those of untreated larvae. Hemocytes of untreated larvae incubating for 30 min with 0.5 mM H_2O_2 were used as the positive control.

2.3.6. Genotoxicity experiments (the comet assay)

DNA damage levels after exposure to PET(Ti)NPLs and TiO_2NPs were determined in hemocytes of *Drosophila* larvae using the single-cell gel electrophoresis (comet assay) as previously described (Alaraby et al., 2020b). Briefly, 3rd instar larvae (72 h) were transferred into a treated medium (31.5, 125, 500 μg/g food) for 24 h. In parallel, wetted medium with Milli-Q water and 4 mM EMS were used as negative and positive controls, respectively. The experiment was performed in triplicate. Hemocytes of about 100 pooled larvae of each dose were collected in clean Eppendorf at 4 °C. To process, 10 μL of hemolymph (contains about ~10,000 hemocytes) was mixed carefully with 90 μL of 0.75% low-melting agarose (at 37 °C) and dropped on the hydrophilic surface of a cold Gelbond film (GBF). After lysis, electrophoresis, neutralization, fixation, and staining, GBFs were mounted, covered with a coverslip, and scored using a Komet 5.5 Image-Analysis System (Kinetic Imaging Ltd., Liverpool, UK) fitted with an Olympus BX50 fluorescence microscope equipped with a 480–550-nm wide-band excitation filter and a 590-nm barrier filter. Three replicates of 100 randomly selected nuclei were analyzed per dose, and the percentage of DNA in the tail (% DNA tail) was used as a measure of DNA damage (Langie et al., 2015).

2.4. Statistical analysis

The IBM SPSS Statistics 21 package was used to statistically analyze the obtained results. Data were analyzed with Kolmogorov-Smirnov & Shapiro-Wilk test and Levene's test to detect their normality and homogeneity (viability data). One-way ANOVA was used to analyze the data with normal distribution and equal variance, while the nonparametric (Mann-Whitney *U* test) was applied for data showing skewed distribution and unequal variance (all data except those of viability). Data were presented in mean ± standard error of the mean (SEM), and the significant differences were calculated at the $P \leq 0.05$ level.

3. Results and discussion

3.1. Characteristics of PET(Ti)NPLs and TiO_2NPs

In this study, titanium-doped PET NPLs were produced by grinding milk PET opaque bottles (Villacorta et al., 2023). To deepen the knowledge of the potential risk of environmental MNPLs, the obtention of true-to-life MNPLs is crucial. In this sense, our results using secondary MNPLs representative of those generated in the environment suppose an important advance. As observed in Supplementary Fig. S1, the obtained nanoplastics showed an irregular shape and a uniform distribution, as detected using high-contrast TEM (Fig. S1A). TEM images showed small black high-electron density dots (corresponding to TiO_2NPs), in addition to the low-contrast PET material. With the help of high-resolution TEM-EDX methodology, the black dots incorporated within the PET matrix were identified as titanium, and with a rod-like shape (Fig. S1E). Interestingly, the morphology and shape of the embedded TiO_2NPs match very well with the rod TiO_2NPs assumed to be used in the production of opaque milk bottles (Fig. S1C). All the above indicated demonstrates the success in obtaining PET NPLs imbibing TiO_2NPs. In using this material, one arising question is whether this hybrid material remains stable over time. In our previous study, we demonstrated that they remain stable both in dispersion and inside the cells since both

signals (PET and Ti) colocalized in both conditions (Villacorta et al., 2023). In addition to determining the potentially harmful effects of these new true-to-life MNPLs, which is the objective of the present study, this type of MNPLs can represent a useful tool to determine the fate of MNPLs inside complex organisms such as mammalian models. In fact, the use of metal-doped nanoplastics was already proposed (Mitrano et al., 2019; Clark et al., 2022), but the proposals use complexes especially synthesized for such ends, and consequently, they cannot be considered representative of the real environmentally MNPLs. This gives special relevance to the use and hazard evaluation of the obtained PET(Ti)NPLs.

3.2. Toxicity and internalization of PET(Ti)NPLs and TiO_2NPs

The first approach when a new compound is tested is to determine its potential toxicity in the used experimental model. In *Drosophila*, the toxic effects measured as the ability of eggs to become an adult were determined, but no toxic effects were detected despite using exposures as high as 500 μg/g food. These doses are based on those used when PET nanoplastics obtained from PET water bottles were used (Alaraby et al., 2023). TiO_2NP exposures were also unable to affect the egg-to-adult viability, despite the high used doses (Supplementary Fig. S2). This lack of a significant toxic effect of TiO_2NPs on *Drosophila* was previously reported by other authors (Carmona et al., 2015; Demir, 2020). It is interesting to point out that the careful examination of the emerged adults did not show any type of morphological abnormalities after exposure to PET(Ti)NPLs or TiO_2NPs (results not shown). Regarding other types of MNPLs, our previous studies indicated that neither polystyrene NPLs (Alaraby et al., 2022a) nor PETNPLs (Alaraby et al., 2023) were able to affect the developmental ability of eggs to reach adult status.

In addition to the potential systemic effects of a defined exposure, the demonstration that the tested agent can be uptake and internalized into the organism is another requirement to be covered in any sound experiment. To obtain this type of information, the *Drosophila* larva is a very useful model since its simple tubular intestine has been recruited to follow the journey of different sorts of nanomaterials (Alaraby et al., 2015; Alaraby et al., 2020). To such end, and using TEM methodologies, the complete internalization pathways of PET(Ti)NPLs (Fig. 1) and TiO_2NPs (Fig. 2) were tracked at the different major compartments (intestinal lumen, intestinal barrier, and hemolymph). Thus, after four days of feeding on a food medium containing PET(Ti)NPLs (500 μg/g food), TEM permitted visualizing the distribution of PET(Ti)NPLs into the larvae midgut lumen (Fig. 1A and B). The presence of Ti was observed very close to symbiotic bacteria (Fig. 1C), crossing their membrane (Fig. 1D), and leading to massive internalization and bacteria death (Fig. 1E). These effects would agree with the observed after TiO_2NPs exposure upon commensal and transient food-borne bacteria especially after chronic exposure, where low levels of gut bacteria were observed (Radziwill-Bienkowska et al., 2018).

Furthermore, PET(Ti)NPLs were observed close to the peritrophic membrane, which simulates the mucus of the mammalian intestine (Fig. 1F), invading the intestinal barrier, and internalizing into midgut enterocytes (Fig. 1G). The presence of PET(Ti)NPLs or TiO_2NPs in microvilli might induce dysfunction and disturbance of gut cells as demonstrated in *in vitro* studies using Caco-2 cells (Faust et al., 2014). Interestingly, when *in vitro* intestinal barrier models, constituted by Caco-2/HT29 cocultures, were exposed to rod TiO_2NPs alterations in the intestinal barrier integrity, were observed (García-Rodriguez et al., 2018). Finally, we observed that PET(Ti)NPLs were able to translocate through the intestinal barrier and deposited in the hemolymph (Fig. 1H), as equivalent to blood in mammals.

Similar results were observed in larvae exposed to TiO_2NPs. Their higher contrast permits a better exploration of their internalization. Taking this advantage, the unstained ultrathin sections showed TiO_2NPs distribution as small black dots at low magnifications in the intestinal lumen, attached to the peritrophic membrane and inside enterocytes (Fig. 2A–C). It was observed the low abundance of symbiotic midgut bacteria of TiO_2NPs treated larvae in comparison with those exposed to PET(Ti)NPL. At this point, it should be remembered that the used PET (Ti)NPLs only contain about 3% of Ti. With the high magnification, TiO_2NPs were observed attached and crossing the peritrophic membrane (Fig. 2D and E) distributed inside the enterocyte's microvilli (Fig. 2F) and accumulated in specific vacuoles (Fig. 2G). Finally, TiO_2NPs penetrated the enterocyte membrane and internalized hemolymph (Fig. 2H).

In addition to TEM, confocal microscopy is also a very relevant tool to visualize PET(Ti)NPLs internalization in the different compartments of the larvae body such as midguts, Malpighian tubes, hemolymph, and

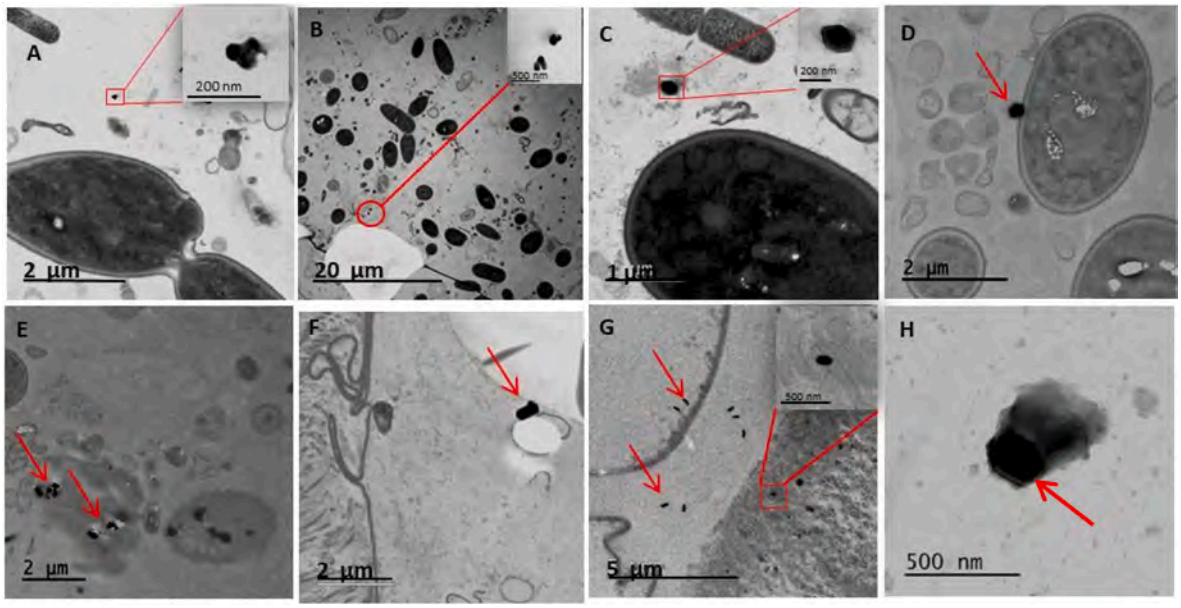

Fig. 1. A complete journey of PET(Ti)NPLs after oral administration until reaching hemolymph (A–H). Particles of PET(Ti)NPLs were distributed in the larvae lumen (A and B), close to or interacting with midgut bacteria (C and D), and inside bacteria (E) or close to the peritrophic membrane (F). PET(Ti)NPLs were able to move inside the microvilli reaching the cytoplasm of enterocytes (G) and, finally, translocated to the hemolymph (H). (E, F, and G, images without contrast).

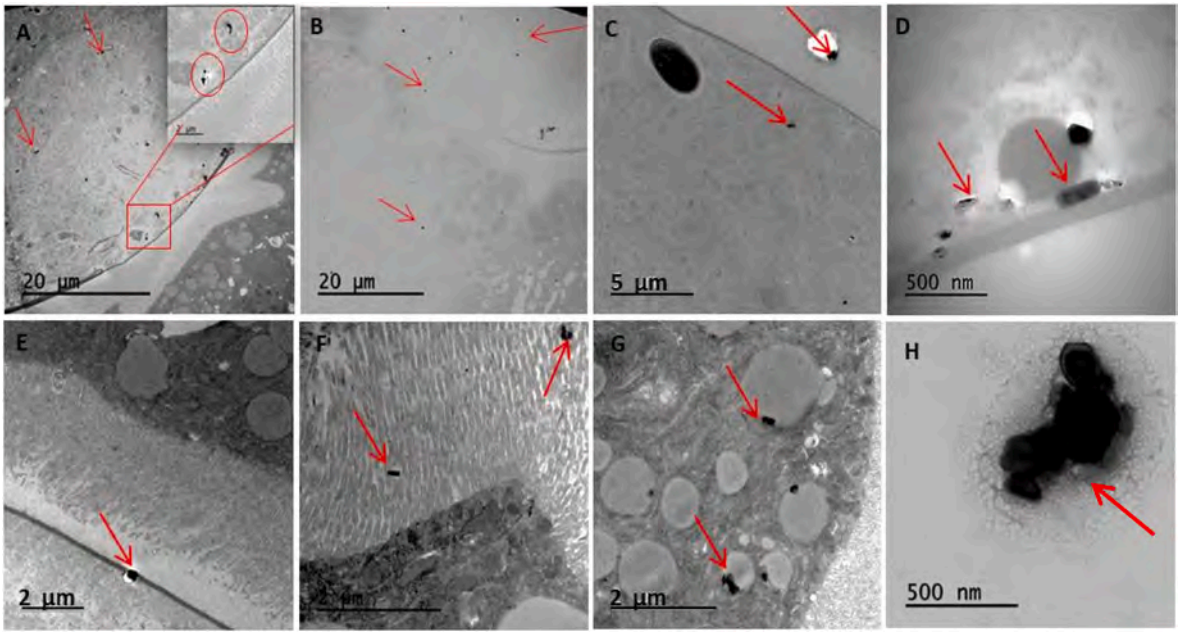

Fig. 2. The complete journey of TiO_2NPs internalization after oral administration, reaching the hemolymph (A–H). With magnification and without contrast, TiO_2NPs appear as small dark dots distributed in the larval lumen (A), and inside enterocytes' cytoplasm (B). TiO_2NPs are visualized on the exterior and interior sides of the peritrophic membrane (C). Interestingly, D and E show the perforation mechanism of TiO_2NPs through the peritrophic membrane. TiO_2NPs are distributed inside microvilli and lysosomes of enterocytes (F and G) and, finally, they reach hemolymph (H).

hemocytes (Fig. 3). Using this approach, differences in colors permit the easy identification of plastic particles from the different cell components. As observed, stained PET showed a green color, while TiO_2NP appeared as white dots using the reflection properties of Ti. In this way, the complex PET(Ti)NPLs produce a twin white/green signal. Using confocal microscopy, the distribution of PET(Ti)NPLs inside midgut cells was detected (Fig. 3a and b). Confocal fluorescent images of midgut cells demonstrated some white/TiO_2NPs signals on the cytoplasm (Fig. 3a), predominance in microvilli (Fig. 3b). Although potentially those signals could reflect some release of Ti from PET(Ti)NPLs, the most probable is

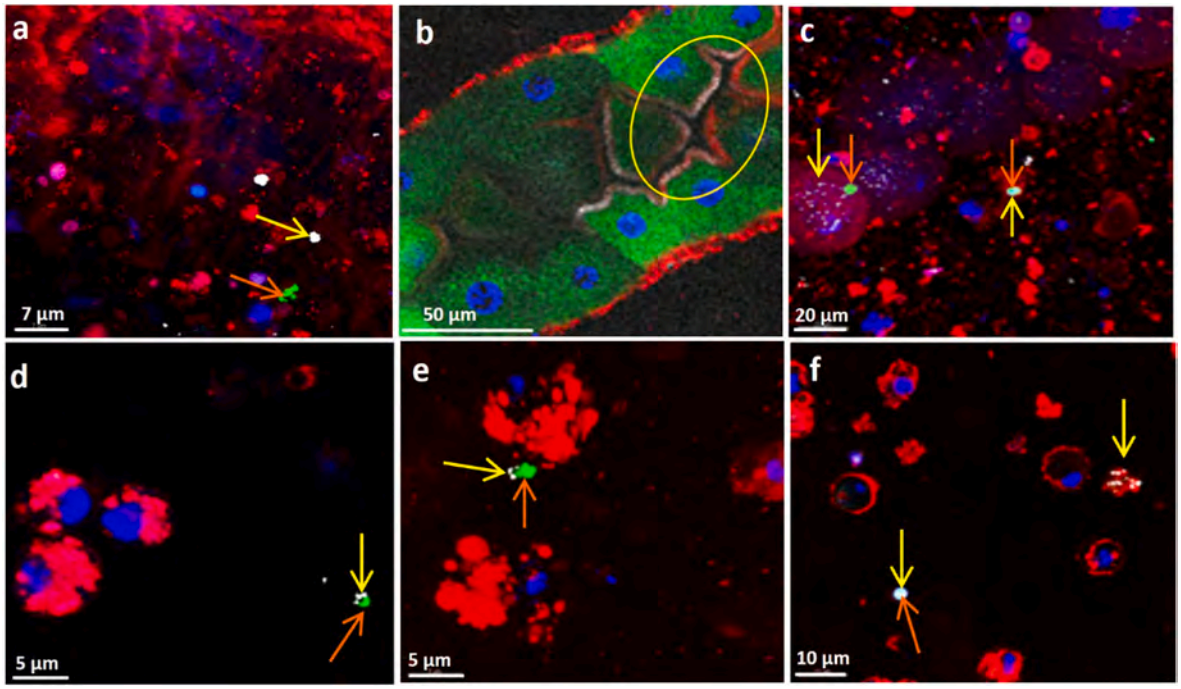

Fig. 3. Fluorescent confocal images showing the internalization of PET(Ti)NPLs in the midgut (a, b), Malpighian tubes (c), and hemolymph including hemocytes (d–f). PET-NPLs show absorption and emission spectra of "green" (orange arrows), while Ti is detected with its reflection property (white dots, yellow arrows). Both particles of PET-NPLs and TiO_2NPs are distributed inside enterocytes' cytoplasm (a), but TiO_2NPs are mainly visualized in the midgut microvilli (b). PET-NPLs and TiO_2NPs are distributed in the cytoplasm of Malpighian tubes with a huge amount of TiO_2NPs inside their lumen (c). PET-NPLs and TiO_2NPs are colocalized and distributed in the hemolymph (d), internalizing hemocytes (e), with Ti signals mainly observed in the hemocytes membrane matrix (f). (For interpretation of the references to color in this figure legend, the reader is referred to the Web version of this article.)

that they represent the real mixture but a small presence of the PET component. However, some PET(Ti)NPLs are distributed very close to the enterocyte nucleus (Fig. a). Interestingly PET(Ti)NPLs were seen inside the Malpighian tubules (Fig. 3c). These tubules constitute the main part of the insect excretory system (Cohen et al., 2020) and are considered part of the renal system since contain multiple cell types and regions and generate primary urine by transcellular transport. Since many genes with key roles in the human kidney have *Drosophila* orthologues, the renal system containing the Malpighian tubules is proposed as a suitable model for studying human kidney pathologies (Dow et al., 2022). Finally, PET(Ti)NPLs were found distributed in hemolymph (Fig. 3d), attached to hemocytes (Fig. 3e), and accumulated inside the hemocytes' cytoplasm and membrane matrix (Fig. 3f).

3.3. Quantification of Ti content in exposed larvae and in the resulting adults

After the qualitative/descriptive presence of PET(Ti)NPLs detected by TEM and confocal microscopy, the presence of Ti in the PET(Ti)NPLs (and obviously in TiO_2NPs) can be quantitatively measured by ICP-MS. To avoid the bias resulting from the PET(Ti)NPLs/TiO_2NPs present in the intestinal tract, the lumen was "cleaned" by moving the exposed larvae to a new food medium (without PET(Ti)NPLs/TiO_2NPs) for 24 h. As expected, significant decreases in the amount of Ti were observed in the "cleaned" larvae regarding those maintained all the time in food containing PET(Ti)NPLs/TiO_2NPs. This was true for both the larvae exposed to PET(Ti)NPLs (Fig. 4A) and for those exposed to TiO_2NPs (Fig. 4B). Interestingly, the observed effects were clearly dose-dependent. Thus, unclean midgut larvae contain 2.0 ± 1.2 and 12.5 ± 2.7 μg/g of titanium, while those with clean midgut have 0.9 ± 0.7 and 2.1 ± 2.2 μg/g after being exposed to 125 and 500 μg/g food of PET (Ti)NPLs (Fig. 4A). It is worth pointing out that the amount of Ti in unclean larvae midgut (12.5 ± 2.7 μg/g) is higher than that located in the food medium (10.5 ± 0.7 μg/g) which would indicate some type of accumulation. Regarding the exposure to TiO_2NPs, the Ti content in unclean midguts larvae was 72.5 ± 12.1 and 347.2 ± 43.1 μg/g after exposures to 125 and 500 μg/g food, which was reduced to 6.4 ± 2.5 and 45.4 ± 10.2 μg/g once the intestine was clean. When the amount of Ti in TiO_2NPs exposed larvae was measured, although the values were much higher than those above indicated, accordingly to the exposure levels, the general internalization behavior was similar (Fig. 4B). The amounts present in the larvae with unclean midgut (347.2 ± 43.1 μg/g) were significantly ($p = 0.017$) higher than those present in the food medium (288.0 ± 9.0 μg/g) wetted with 500 μg/g food TiO_2NPs. This would confirm the accumulation of Ti by the exposed larvae, possibly in the Malpighian tubules (Fig. 3d-e).

It is interesting to point out the results obtained with the adults resulting from the exposed larvae when the amounts of Ti in their bodies were determined. It should be remembered that *Drosophila* is an insect with complex metamorphosis where larvae after reaching the third instar, became pupae where all tissues are destroyed, and the adult is constituted from the primordial cells constituting the different imaginal disks of the larvae (Hall and Martín-Vega, 2019). The obtained levels of Ti in the adults were 1.3 ± 0.9 and 3.4 ± 3.2 μg/g when they were exposed during the larval stage to 125 and 500 μg/g food of PET(Ti) NPLs. Analogously, the values were 15.4 ± 7.8 and 30.5 ± 10.0 μg/g for adults emerging from larvae exposed to 125 and 500 μg/g food of TiO_2NPs (Fig. 4C). Unfortunately, no studies have been found quantifying the levels of metal nanoparticles in the exposed larvae and in the resulting adults. Nevertheless, our results would explain the results obtained in larvae exposed to AgNPs where high levels of this nanometal were determined inside the pupae. In such cases, although the levels of AgNPs were not determined in adults, the effects observed in the development of adults as well as ROS-mediated stress responses were attributed to the exposure in the pupae larvae stage (Mao et al., 2018). However, the exitance of Ti in flies' tissues could mediate development impacts. In this regard, TiO_2NPs significantly reduced the progeny of the fruit fly through declining female fecundity (Philbrook et al., 2011). Further research should be designed to highlight the impacts of metal nanoparticles, especially those doped plastic products, across different generations after exposure.

It is remarkable to point out that the accumulation of TiO_2NPs in the larval body is dependent on the shape, with nanorod levels being higher than those of nanowires or nanospheres under equivalent exposure doses, as observed by Alaraby et al. (2021). It should be remembered that titanium nanorods were those constituting the PET(Ti)NPLs and the TiO_2NPs used in this study. Furthermore, the observed accumulation of Ti in the body is relevant mainly under chronic exposure scenarios, as used in our study where larvae were exposed all their life until they reach the pupae stage. In fact, this bioaccumulation inside the gut was already reported in rats exposed to relatively low doses of TiO_2NPs (Ammendolia et al., 2017). Similarly, in several marine bivalve mollusks the internal levels of different metals, including Ti nanomaterials, were higher than the concentration measured in seawater (Xu et al., 2020).

3.4. Molecular responses to PET(Ti)NPLs and TiO_2NPs exposures

The internalization of xenobiotic agents can affect cell homeostasis and these effects can be manifested immediately after exposure, as changes in the expression levels of genes involved in different pathways.

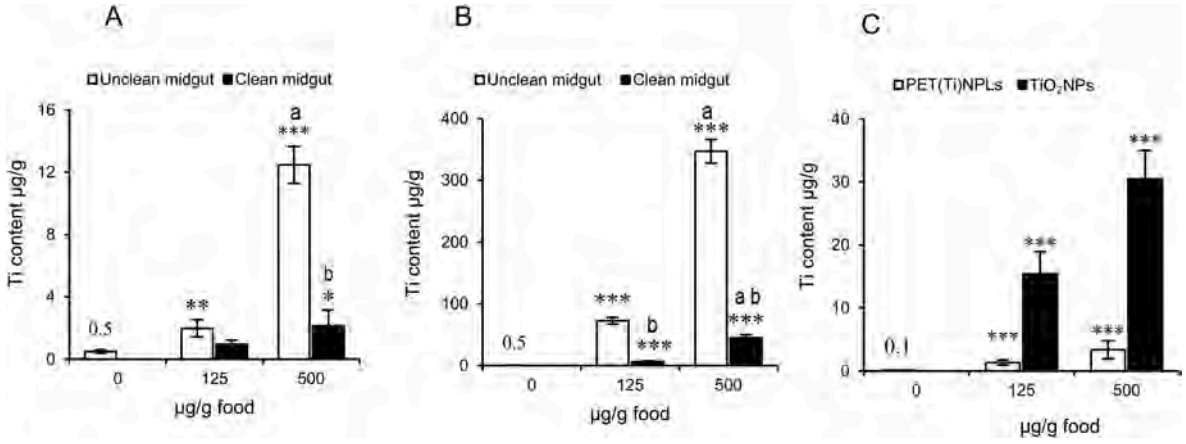

Fig. 4. The titanium content in larvae exposed to PET(Ti)NPLs (A), to TiO_2NPs (B), and in the resulting adults (C). *$P < 0.05$, **$P < 0.01$, ***$P < 0.001$ (exposed *vs* unexposed). (a) Indicates significant differences between doses (500 *vs* 125 μg/g food) and (b) indicates significant differences between larvae with clean and unclean midguts for the same concentration (Mann-Whitney *U* test).

Latter effects can occur depending on different factors including the exposure levels. For such reason, the use of one battery of genes involved in the general response to xenobiotics should be included to identify the quick response of the tested organism to a defined exposure. It is worth mentioning that according to the selected genes, information on the involved mechanisms of action can also be reached following this approach. In our case, we have selected eight genes involved in different pathways These genes are considered a standard battery that has proved to be useful in detecting the harmful effects induced by nanoparticles (Alaraby et al., 2021) and nanoplastics (Alaraby et al., 2020b). The obtained results are presented in Fig. 5.

As observed, the heat shock protein (*Hsp70*) gene was significantly down-regulated for both compounds regardless of the dose, with a slightly higher impact after PET(Ti)NPLs exposure. The two genes regulating the expression of antioxidant enzymes (*Cat* and *Sod2*) were also deregulated, but in the opposite direction since while *Cat* expression was down-regulated, *Sod2* expression was up-regulated in a dose-dependent manner after exposures to PET(Ti)NPLs or TiO_2NPs; the effects induced by TiO_2NPs being more marked. Regarding the effects induced on the expression levels of the DNA repair gene (*Ogg1*), they were significantly de-regulated with different doses of both PET(Ti)NPLs and TiO_2NPs. Finally, the selected genes modulating the integrity of the intestinal barrier (*Duox* and *Peri*) showed significant de-regulation but, while the expression of *Duox* showed an upward trend, *Peri* expression was downregulated with all doses of both tested agents.

Herein we have detected the ability of PET(Ti)NPLs to deregulate various response pathways at all studied doses, in a similar way that was observed with TiO_2NPs exposures. It is remarkable the dose-dependent increases observed in the expression of *Sod2* after the exposure to TiO_2NPs which could be attributed to the effect of the metal itself, as it was observed when *Drosophila* was exposed to different metals, such as aluminum (Wu et al., 2012), AgNPs (Alaraby et al., 2019), and CdONPs (El Kholy et al., 2021). Increases, although not at these high levels, were also observed in the larvae exposed to PET(Ti)NPLs. Although these lower increases could be attributed to the low concentration of Ti, it must be pointed out that *Sod2* expression was observed to be significantly increased after exposures to PET-NPLs obtained from PET water bottles (Alaraby et al., 2023). Another important finding is the over-expression of *Duox*, which is a ROS-producing nicotinamide adenine dinucleotide phosphate (NADPH) oxidase, involved in the generation of hydrogen peroxide and acts as the innate immune response strategy to combat pathogens, as occurs also in humans (Capo et al., 2019). This would indicate that exposure to PET(Ti)NPLs is causing severe effects on the gut microbiome since *Duox* acts as a good sensor of microbiota dysbiosis involved in maintaining intestinal homeostasis in insects (Yao et al., 2016).

3.5. Oxidative stress induction by PET(Ti)NPLs and TiO_2NPs exposures

To highlight the potential ability of Ti-doped NPLs, as well as TiO_2NPs, to increase the intracellular ROS levels, hemocytes of the exposed larvae were examined using DCFH-DA, as a well-accepted ROS probe. Fluorescent representative images were analyzed and the obtained data are drawn in Fig. 6A. As observed, both PET(Ti)NPLs and TiO_2NPs induced elevated levels of oxidative stress in a dose-dependent manner, reaching about 9.5 folds at the highest dose (500 μg/g food) of both compounds, with respect to background ROS levels observed in untreated flies. The lower doses of PET(Ti)NPLs caused more ROS induction (especially at 31.5 μg/g food) than those induced by TiO_2NPs. It should be remembered that the levels of TiO_2NPs in PET(Ti)NPLs are only 3% which indicates that the effects of the complex are basically induced by the PET component.

Among the most abundant ROS, superoxide stands out and SOD enzymes catalyze its breakdown into hydrogen peroxide and water (Landis and Tower, 2005). Although the up-regulation of *Sod2* aims to reduce the oxidative stress levels, it was insufficient to overcome the excessive ROS generated by the exposure (Petković et al., 2011) which would explain the high level of intracellular ROS observed in hemocytes

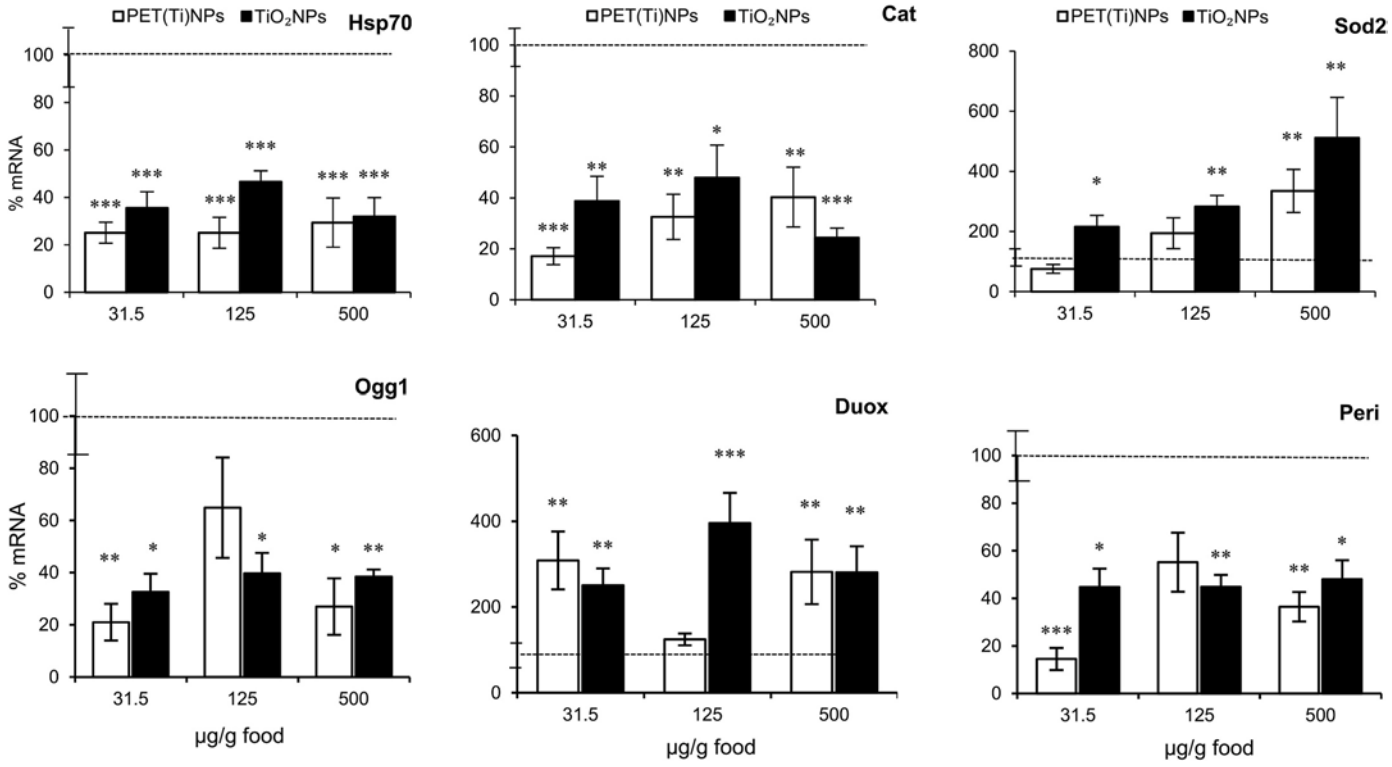

Fig. 5. The molecular response of larvae treated with PET(Ti)NPLs and TiO_2NPs. The expression of different genes including general stress (*Hsp70*), oxidative stress (*Cat* and *Sod2*), DNA repair (*Ogg1),* and intestinal physical stress (*Duox, Peri*) genes was determined. The horizontal dotted line corresponds to the control values. Relative values are expressed. $^*P < 0.05$, $^{**}P < 0.01$, $^{***}P < 0.001$ (Mann-Whitney *U* test).

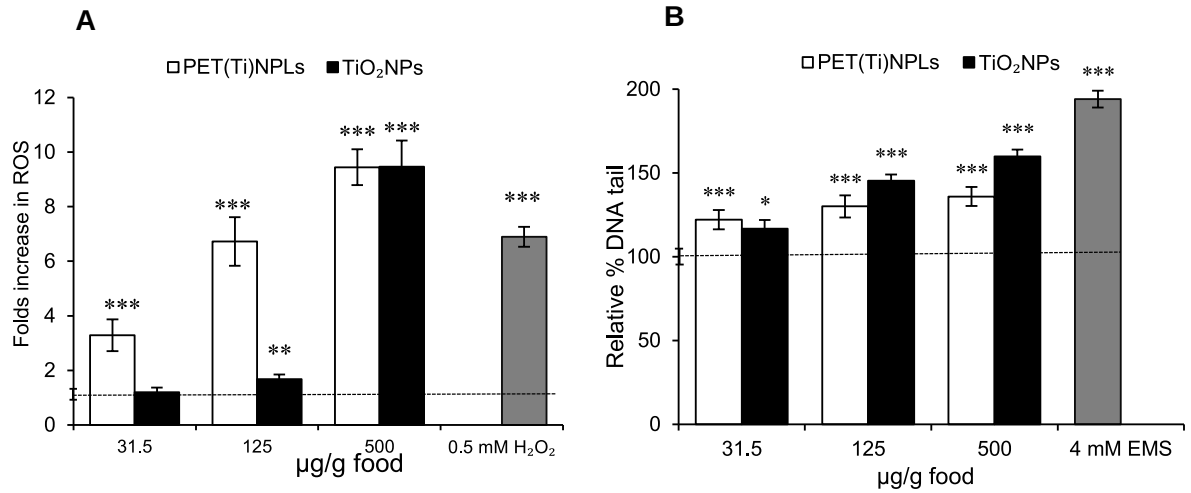

Fig. 6. (A) Oxidative stress produced in *Drosophila* larvae hemocytes exposed to different doses of PET(Ti)NPLs and TiO_2NPs. (B) Percentage of DNA damage in *Drosophila* larvae' hemocytes exposed to different doses of PET(Ti)NPLs or TiO_2NPs. The horizontal dotted line corresponds to the control values. $^*P < 0.05$, $^{**}P < 0.01$, and $^{***}P < 0.001$ (Mann-Whitney *U* test was used to analyze the data with non-homogenous variance).

after exposures to both PET(Ti)NPLs and TiO_2NPs. Furthermore, the observed downregulation of the *cat* gene could also be correlated to an increase in the generation of ROS.

It is assumed that the main mechanism underlining the toxic potential of TiO_2NPs involves ROS production (Grande and Tucci, 2016). In fact, the only two studies using Drosophila and testing ROS levels induced by TiO2NPs observed significant increases in such levels (Demir, 2020; Alaraby et al., 2021). Interestingly, TiO_2NPs exposure alters glucose transport across the intestinal epithelium, damaging intestinal microvilli (Richter et al., 2018) and this would explain the overexpression of *Duox* as a response to gut damage which, in turn, would explain the high levels of ROS. Nevertheless, the ROS induced by PET(Ti)NPLs cannot be attributed only to the TiO_2NPs since PETNPLs were reported to induce ROS in human primary nasal epithelial cells used as a model of the first barrier of the respiratory system (Annangi et al., 2023).

3.6. DNA damage induction by PET(Ti)NPLs and TiO_2NPs exposures

The ability of PET(Ti)NPLs and TiO_2NPs to induce DNA damage was explored in hemocytes of *Drosophila* larvae using the comet assay, as a tool to detect DNA breaks. As observed in Fig. 6B both, PET(Ti)NPLs and TiO_2NPs were able to induce significant increases in the levels of DNA damage. Interestingly, the observed effects were dose-dependent, with higher genotoxic effects associated with TiO_2NPs exposure.

Among the different harmful effects induced by environmental agents, the ability to damage DNA stands out. This is because it is well known the a strong association between DNA damage induction and drastic health consequences for humans (Carbone et al., 2020). Accordingly, determining the genotoxic effects induced by exposure is of special relevance. The genotoxicity of titanium compounds, including Ti nanoparticles, is a controversial issue mainly due to the recent position of the European Food Safety Authority (EFSA) announcing that it is not possible to rule out the genotoxicity from titanium dioxide and therefore it "can no longer be considered as safe when used as a food additive" (EFSA, 2021). In this context, our results showing the ability of TiO_2NPs to induce DNA damage in *Drosophila* acquire a special relevance. It must be stated that different shapes of TiO_2NPs have been shown to exert genotoxicity in *Drosophila* using different approaches (Demir, 2020; Alaraby et al., 2021), and when flies were exposed to doses simulating the estimated daily consumption concentration in humans in a long-term exposure scenario lasting for 20 generations (Jovanović et al., 2018).Our positive results in the genotoxicity assessment agree with the observed increased levels of oxidative stress induced by TiO_2NPs, although it has been proposed that the genotoxicity would be a secondary effect of the induced physiological stress more than a direct effect on DNA (Kirkland et al., 2022).

Regarding the positive genotoxic effects induced by PET(Ti)NPLs they could be attributed to the TiO_2NPs, but the effect of the plastic itself cannot be discarded. The genotoxic potential of MNPLs is under discussion, although some examples point out genotoxic effects. Focusing on true-to-life PETNPLs, two recent papers have recorded genotoxic data in cell cultures. In a preliminary study using monocytic THP1 cells, PETNPLs resulting from sanding commercial water PET bottles do not exert genotoxic effects in the comet assay (Villacorta et al., 2022). This lack of effects can be attributed to the short exposure time (3 h) and the relatively low concentration (50 µg/mL) used, although possibly also to the used cell lines. Thus, when THP-1 cells were differentiated to macrophage-like cells they showed more sensitivity to polystyrene MNPLs exposures (Visalli et al., 2023). On the other side, using PETNPL samples obtained by grinding transparent plastic food containers, significant increases in the levels of strand breaks were observed in Caco-2 and HepG2 cells (Roursgaard et al., 2022). Finally, the testing of the PETNPLs resulting from sanding commercial water bottles induced both oxidative stress and DNA damage induction (comet assay) when tested in *Drosophila* (Alaraby et al., 2023).

4. Conclusions

The presence of TiO_2NPs embedded in the PET polymer of opaque milk bottles was confirmed with TEM and ICP-MS methodologies. The TiO_2NPs of PET(Ti)NPLs have a similar diameter to that of selected nanorod(TiO_2NPs) evaluated in parallel, which would confirm their chemical nature and shape. Interestingly, these PET(Ti)NPLs have shown their suitability to follow their journey inside the larval body, with a negative impact on the abundance of commensal microbiota and reaching the hemolymph compartment, once translocated the intestinal barrier. In addition to tracking their presence in the body, PET(Ti)NPLs have been shown to be useful in quantifying their internalization permitting observing their bioaccumulation inside the body, mainly in the excretory organs such as the Malpighian tubules. Both PET(Ti)NPLs and TiO_2NPs were able to produce a wide range of hazardous effects by altering gene expression of different response pathways, producing dose-dependent oxidative stress and DNA damage. Interestingly, those effects induced by PET(Ti)NPLs were not completely attributed to the TiO_2NPs component, and the role of PETNPLs cannot be ruled out. True-

to-life MNPLs as those used in this study can be used for many purposes such as to easily detect/quantify their presence in different tissues and organs of complex organisms such as in experimental mammalian models.

Author contribution statement

RM, AH, and MA planned the experiments. MA, DA, and AV performed the experiments. MA did the statistical analysis of the obtained data as well as prepared figures. MA, AH, and RM wrote the final manuscript.

Declaration of competing interest

The authors declare that they have no known competing financial interests or personal relationships that could have appeared to influence the work reported in this paper.

Data availability

Data will be made available on request.

Acknowledgments

M. Alaraby holds a Maria Zambrano postdoctoral contract (code 693063) from the *Ministerio de Universidades,* funded by the European Union-Next GenerationEU, at the UAB. A. Villacorta was supported by a PhD fellowship from the National Agency for Research and Development (ANID), CONICYT PFCHA/DOCTORADO BECAS CHILE/2020–72210237. D. Abass was a Visitor Researcher at the UAB. A. Hernández was granted an ICREA ACADEMIA award.

The PlasticHeal project has received funding from the European Union's Horizon 2020 research and innovation programme under grant agreement No 965196. This study was supported by the Spanish Ministry of Science and Innovation (PID 2020-116789RB-C43) and the Generalitat de Catalunya (2021-SGR-00731).

We thank the Molecular Spectroscopy and Optical Microscopy facility (ICN2) for using their facilities.

Appendix A. Supplementary data

Supplementary data to this article can be found online at https://doi.org/10.1016/j.envpol.2023.122968.

References

Alaraby, M., Abass, D., Domenech, J., Hernández, A., Marcos, R., 2022a. Hazard assessment of ingested polystyrene nanoplastics in *Drosophila* larvae. Environ. Sci.: Nano 9 (5), 1845–1857. https://doi.org/10.1039/D1EN01199E.

Alaraby, M., Abass, D., Villacorta, A., Hernández, A., Marcos, R., 2022b. Antagonistic *in vivo* interaction of polystyrene nanoplastics and silver compounds. A study using *Drosophila*. Sci. Total Environ. 842, 156923 https://doi.org/10.1016/j.scitotenv.2022.156923.

Alaraby, M., Annangi, B., Hernández, A., Creus, A., Marcos, R., 2015. A comprehensive study of the harmful effects of ZnO nanoparticles using *Drosophila melanogaster* as an *in vivo* model. J. Hazard Mater. 296, 166–174. https://doi.org/10.1016/j.jhazmat.2015.04.053.

Alaraby, M., Hernández, A., Marcos, R., 2018. Systematic *in vivo* study of NiO nanowires and nanospheres: biodegradation, uptake, and biological impacts. Nanotoxicology 12 (9), 1027–1044. https://doi.org/10.1080/17435390.2018.1513091.

Alaraby, M., Romero, S., Hernández, A., Marcos, R., 2019. Toxic and genotoxic effects of silver nanoparticles in *Drosophila*. Environ. Mol. Mutagen. 60 (3), 277–285. https://doi.org/10.1002/em.22262.

Alaraby, M., Demir, E., Domenech, J., Velázquez, A., Hernández, A., Marcos, R., 2020. *In vivo* evaluation of the toxic and genotoxic effects of exposure to cobalt nanoparticles using *Drosophila melanogaster*. Environ. Sci.: Nano 7 (2), 610–622. https://doi.org/10.1039/C9EN00690G.

Alaraby, M., Hernández, A., Marcos, R., 2021. Novel insights into biodegradation, interaction, internalization and impacts of high-aspect-ratio TiO_2 nanomaterials: a systematic *in vivo* study using *Drosophila melanogaster*. J. Hazard Mater. 409, 124474 https://doi.org/10.1016/j.jhazmat.2020.124474.

Alaraby, M., Villacorta, A., Abass, D., Hernández, A., Marcos, R., 2023. The hazardous impact of true-to-life PET nanoplastics in *Drosophila*. Sci. Total Environ. 863, 160954 https://doi.org/10.1016/j.scitotenv.2022.160954.

Ammendolia, M.G., Iosi, F., Maranghi, F., Tassinari, R., Cubadda, F., Aureli, F., Raggi, A., Superti, F., Mantovani, A., De Berardis, B., 2017. Short-term oral exposure to low doses of nano-sized TiO_2 and potential modulatory effects on intestinal cells. Food Chem. Toxicol. 102, 63–75. https://doi.org/10.1016/j.fct.2017.01.031.

Annangi, B., Villacorta, A., Vela, L., Tavakolpournegari, A., Marcos, R., Hernández, A., 2023. Effects of true-to-life PET nanoplastics using primary human nasal epithelial cells. Environ. Toxicol. Pharmacol. 100, 104140. https://doi.org/10.1016/j.etap.2023.104140.

Barguilla, I., Domenech, J., Rubio, L., Marcos, R., Hernández, A., 2022. Nanoplastics and arsenic co-exposures exacerbate oncogenic biomarkers under an *in vitro* long-term exposure scenario. Int. J. Mol. Sci. 23 (6), 2958. https://doi.org/10.3390/ijms23062958.

Buchon, N., Silverman, N., Cherry, S., 2014. Immunity in *Drosophila melanogaster* -from microbial recognition to whole-organism physiology. Nat. Rev. Immunol. 14 (12), 796–810. https://doi.org/10.1038/nri3763.

Capo, F., Wilson, A., Di Cara, F., 2019. The intestine of Drosophila melanogaster: an emerging versatile model system to study intestinal epithelial homeostasis and host-microbial interactions in humans. Microorganisms 7 (9), 336. https://doi.org/10.3390/microorganisms7090336.

Carbone, M., Arron, S.T., Beutler, B., Bononi, A., Cavenee, W., Cleaver, J.E., Croce, C.M., D'Andrea, A., Foulkes, W.D., Gaudino, G., Groden, J.L., Henske, E.P., Hickson, I.D., Hwang, P.M., Kolodner, R.D., Mak, T.W., Malkin, D., Monnat Jr., R.J., Novelli, F., Pass, H.I., Petrini, J.H., Schmidt, L.S., Yang, H., 2020. Tumour predisposition and cancer syndromes as models to study gene-environment interactions. Nat. Rev. Cancer 20 (9), 533–549. https://doi.org/10.1038/s41568-020-0265-y.

Carmona, E.R., Escobar, B., Vales, G., Marcos, R., 2015. Genotoxic testing of titanium dioxide anatase nanoparticles using the wing-spot test and the comet assay in *Drosophila*. Mutat. Res. 778, 12–21. https://doi.org/10.1016/j.mrgentox.2014.12.004.

Clark, N.J., Khan, F.R., Mitrano, D.M., Boyle, D., Thompson, R.C., 2022. Demonstrating the translocation of nanoplastics across the fish intestine using palladium-doped polystyrene in a salmon gut-sac. Environ. Int. 159, 106994 https://doi.org/10.1016/j.envint.2021.106994.

Cohen, E., Sawyer, J.K., Peterson, N.G., Dow, J.A.T., Fox, D.T., 2020. Physiology, development, and disease modeling in the Drosophila excretory system. Genetics 214 (2), 235–264. https://doi.org/10.1534/genetics.119.302289.

Demir, E., 2020. An in vivo study of nanorod, nanosphere, and nanowire forms of titanium dioxide using Drosophila melanogaster: toxicity, cellular uptake, oxidative stress, and DNA damage. J. Toxicol. Environ. Health A. 83 (11–12), 456–469. https://doi.org/10.1080/15287394.2020.1777236.

Domenech, J., Cortés, C., Vela, L., Marcos, R., Hernández, A., 2021. Polystyrene nanoplastics as carriers of metals. Interactions of polystyrene nanoparticles with silver nanoparticles and silver nitrate, and their effects on human intestinal Caco-2 cells. Biomolecules 11 (6), 859. https://doi.org/10.3390/biom11060859.

Dow, J.A.T., Simons, M., Romero, M.F., 2022. *Drosophila melanogaster:* a simple genetic model of kidney structure, function and disease. Nat. Rev. Nephrol. 18 (7), 417–434. https://doi.org/10.1038/s41581-022-00561-4.

Ducoli, S., Federici, S., Nicsanu, R., Zendrini, A., Marchesi, C., Paolini, L., Radeghieri, A., Bergese, P., Depero, L.E., 2022. A different protein corona cloaks "true-to-life" nanoplastics with respect to synthetic polystyrene nanobeads. Environ. Sci.: Nano 9 (4), 414–1426. https://doi.org/10.1039/D1EN01016F.

El Kholy, S., Giesy, J.P., Al Naggar, Y., 2021. Consequences of a short-term exposure to a sub lethal concentration of CdO nanoparticles on key life history traits in the fruit fly (Drosophila melanogaster). J. Hazard. Mater. 410, 124671. https://doi.org/10.1016/j.jhazmat.2020.124671.

Faust, J.J., Doudrick, K., Yang, Y., Westerhoff, P., Capco, D.G., 2014. Food grade titanium dioxide disrupts intestinal brush border microvilli in vitro independent of sedimentation. Cell. Biol. Toxicol. 30 (3), 169–188. https://doi.org/10.1007/s10565-014-9278-1.

Flavourings (FAF), Younes, M., Aquilina, G., Castle, L., Engel, K.H., Fowler, P., Frutos Fernandez, M.J., Fürst, P., Gundert-Remy, U., Gürtler, R., Husøy, T., EFSA, Panel on Food Additives, 2021. Safety assessment of titanium dioxide (E171) as a food additive. Efsa J. 19 (5), e06585. https://doi.org/10.2903/j.efsa.2021.6585.

García-Rodríguez, A., Vila, L., Cortés, C., Hernández, A., Marcos, R., 2018. Effects of differently shaped TiO_2NPs (nanospheres, nanorods, and nanowires) on the *in vitro* model (Caco-2/HT29) of the intestinal barrier. Part. Fibre Toxicol. 15 (1), 33. https://doi.org/10.1186/s12989-018-0269-x.

Grande, F., Tucci, P., 2016. Titanium dioxide nanoparticles: a risk for human health? Mini Rev. Med. Chem. 16 (9), 762–769. https://doi.org/10.2174/1389557516666160321114341.

Hall, M.J.R., Martín-Vega, D., 2019. Visualization of insect metamorphosis. Philos. Trans. R. Soc. Lond. B Biol. Sci. 374 (1783), 20190071 https://doi.org/10.1098/rstb.2019.0071.

Jovanović, B., Jovanović, N., Cvetković, V.J., Matić, S., Stanić, S., Whitley, E.M., Mitrović, T.L., 2018. The effects of a human food additive, titanium dioxide nanoparticles E171, on *Drosophila melanogaster* -a 20 generation dietary exposure experiment. Sci. Rep. 8 (1), 17922 https://doi.org/10.1038/s41598-018-36174-w.

Kirkland, D., Aardema, M.J., Battersby, R.V., Beevers, C., Burnett, K., Burzlaff, A., Czich, A., Donner, E.M., Fowler, P., Johnston, H.J., Krug, H.F., Pfuhler, S., Stankowski Jr., L.F., 2022. A weight of evidence review of the genotoxicity of titanium dioxide (TiO_2). Regul. Toxicol. Pharmacol. 136, 105263 https://doi.org/10.1016/j.yrtph.2022.105263.

Landis, G.N., Tower, J., 2005. Superoxide dismutase evolution and life span regulation. Mech. Ageing Dev. 126 (3), 365–379. https://doi.org/10.1016/j.mad.2004.08.012.

Langie, S.A., Azqueta, A., Collins, A.R., 2015. The comet assay: past, present, and future. Front. Genet. 6, 266. https://doi.org/10.3389/fgene.2015.00266.

Mao, B.H., Chen, Z.Y., Wang, Y.J., Yan, S.J., 2018. Silver nanoparticles have lethal and sublethal adverse effects on development and longevity by inducing ROS-mediated stress responses. Sci. Rep. 8 (1), 2445. https://doi.org/10.1038/s41598-018-20728-z.

Marchesi, C., Rani, M., Federici, S., Alessandri, I., Vassalini, I., Ducoli, S., Borgese, L., Zacco, A., Núñez-Delgado, A., Bontempi, E., Depero, L.E., 2023. Quantification of ternary microplastic mixtures through an ultra-compact near-infrared spectrometer coupled with chemometric tools. Environ. Res. 216 (Pt 3), 114632 https://doi.org/10.1016/j.envres.2022.114632.

Mitrano, D.M., Beltzung, A., Frehland, S., Schmiedgruber, M., Cingolani, A., Schmidt, F., 2019. Synthesis of metal-doped nanoplastics and their utility to investigate fate and behaviour in complex environmental systems. Nat. Nanotechnol. 14 (4), 362–368. https://doi.org/10.1038/s41565-018-0360-3.

Petković, J., Zegura, B., Stevanović, M., Drnovšek, N., Uskoković, D., Novak, S., Filipič, M., 2011. DNA damage and alterations in expression of DNA damage responsive genes induced by TiO_2 nanoparticles in human hepatoma HepG2 cells. Nanotoxicology 5 (3), 341–353. https://doi.org/10.3109/17435390.2010.507316.

Philbrook, N.A., Winn, L.M., Afrooz, A.N., Saleh, N.B., Walker, V.K., 2011. The effect of TiO_2 and Ag nanoparticles on reproduction and development of *Drosophila melanogaster* and CD-1 mice. Toxicol. Appl. Pharmacol. 257 (3), 429–436. https://doi.org/10.1016/j.taap.2011.09.027.

Radziwill-Bienkowska, J.M., Talbot, P., Kamphuis, J.B., Robert, V., Cartier, C., Fourquaux, I., Lentzen, E., Audinot, J.N., Jamme, F., Réfrégiers, M., Bardowski, J.K., 2018. Toxicity of food-grade TiO_2 to commensal intestinal and transient food-borne bacteria: new insights using nano-SIMS and synchrotron UV fluorescence imaging. Front. Microbiol. 9, 794. https://doi.org/10.3389/fmicb.2018.00794.

Reiter, L.T., Potocki, L., Chien, S., Gribskov, M., Bier, E., 2001. A systematic analysis of human disease-associated gene sequences in *Drosophila melanogaster*. Genome Res. 11, 1114–1125. https://doi.org/10.1101/gr.169101.

Richter, J.W., Shull, G.M., Fountain, J.H., Guo, Z., Musselman, L.P., Fiumera, A.C., Mahler, G.J., 2018. Titanium dioxide nanoparticle exposure alters metabolic homeostasis in a cell culture model of the intestinal epithelium and *Drosophila melanogaster*. Nanotoxicology 12 (5), 390–406. https://doi.org/10.1080/17435390.2018.1457189.

Roursgaard, M., Hezareh Rothmann, M., Schulte, J., Karadimou, I., Marinelli, E., Møller, P., 2022. Genotoxicity of particles from grinded plastic items in Caco-2 and HepG2 Cells. Front. Public Health 10, 906430. https://doi.org/10.3389/fpubh.2022.906430.

Rubin, G.M., Yandell, M.D., Wortman, J.R., Gabor Miklos, G.L., Nelson, C.R., Hariharan, I.K., Fortini, M.E., Li, P.W., Apweiler, R., Fleischmann, W., et al., 2000. Comparative genomics of the eukaryotes. Science 287 (5461), 2204–2215. https://doi.org/10.1126/science.287.5461.2204.

Su, Y., Hu, X., Tang, H., Lu, K., Li, H., Liu, S., Xing, B., Ji, R., 2022. Steam disinfection releases micro (nano) plastics from silicone-rubber baby teats as examined by optical photothermal infrared microspectroscopy. Nat. Nanotechnol. 17 (1), 76–85. https://doi.org/10.1038/s41565-021-00998-x.

Villacorta, A., Rubio, L., Alaraby, M., López-Mesas, M., Fuentes-Cebrian, V., Moriones, O. H., Marcos, R., Hernández, A., 2022. A new source of representative secondary PET nanoplastics. Obtention, characterization, and hazard evaluation. J. Hazard Mater. 439, 129593 https://doi.org/10.1016/j.jhazmat.2022.129593.

Villacorta, A., Vela, L., Morataya-Reyes, M., Llorens-Chiralt, R., Rubio, L., Alaraby, M., Marcos, R., Hernández, A., 2023. Titanium-doped PET nanoplastics of environmental origin as a true-to-life model of nanoplastics. Sci. Total Environ. 880, 163151 https://doi.org/10.1016/j.scitotenv.2023.163151.

Visalli, G., Laganà, A., Facciolà, A., Iaconis, A., Curcio, J., Pollino, S., Celesti, C., Scalese, S., Libertino, S., Iannazzo, D., Di Pietro, A., 2023. Enhancement of biological effects of oxidised nano- and microplastics in human professional phagocytes. Environ. Toxicol. Pharmacol. 99, 104086 https://doi.org/10.1016/j.etap.2023.104086.

Wu, Z., Du, Y., Xue, H., Wu, Y., Zhou, B., 2012. Aluminum induces neurodegeneration and its toxicity arises from increased iron accumulation and reactive oxygen species (ROS) production. Neurobiol. Aging 33 (1). https://doi.org/10.1016/j.neurobiolaging.2010.06.018, 199.e1-12.

Xu, L., Wang, Z., Zhao, J., Lin, M., Xing, B., 2020. Accumulation of metal-based nanoparticles in marine bivalve mollusks from offshore aquaculture as detected by single particle ICP-MS. Environ. Pollut. 260, 114043 https://doi.org/10.1016/j.envpol.2020.114043.

Yao, Z., Wang, A., Li, Y., Cai, Z., Lemaitre, B., Zhang, H., 2016. The dual oxidase gene *BdDuox* regulates the intestinal bacterial community homeostasis of *Bactrocera dorsalis*. ISME J. 10, 1037–1050. https://doi.org/10.1038/ismej.2015.202, 2016.